ELSEVIER

Chemical Engineering Journal 129 (2007) 91–103

Chemical Engineering Journal

www.elsevier.com/locate/cej

Variable density fluid reactor network synthesis—Construction of the attainable region through the IDEAS approach

Wen Zhou, Vasilios I. Manousiouthakis*

Chemical Engineering Department, University of California, Los Angeles Los Angeles, CA 90095, United States

Received 27 April 2006; received in revised form 3 November 2006; accepted 8 November 2006

Abstract

In this work, the *I*nfinite *D*im*E*nsion*A*l *S*tate-space (IDEAS) method and the associated Shrink-wrap algorithm are shown to be applicable to variable density fluid (VDF) reactor network synthesis (RNS). To this end, mathematical models for variable density fluid continuous stirred tank reactors (CSTR) and plug flow reactors (PFR) are shown to give rise to linear operators within the IDEAS framework. Using IDEAS, a variety of convex (linear) objective functions, such as maximization of concentration, yield, selectivity, or economic considerations like minimization of total reactor volume, or attainable region construction can be handled by linear programming. To demonstrate the effectiveness of the proposed method, three reactor network synthesis case studies involving gas phase reactions are presented.

Keywords: Reactor network synthesis; Variable density fluid reactor; IDEAS

1. Introduction

Reactors and reactor networks are crucial to the success of a chemical plant. Consequently, the analysis and design of reactors and reactor networks have been one of the focal points of Process Systems Engineering (PSE). At the education level, Gavalas, Levenspiel, Froment and Bischoff, Fogler, Schmidt, and Rawlings and Ekerdt addressed reactor analysis and design, while Levenspiel, Fogler, and Rawlings and Ekerdt also addressed reactor network analysis and design [1–6]. At the research level, superstructure optimization and attainable region (AR) construction have been the main tools for reactor network synthesis (RNS).

The initial concept of superstructure dates back to the sixties, when Jackson studied a network of parallel PFRs interconnected with sidestreams [7]. A number of different superstructure models were investigated and a variety of solution methodologies for the resulting optimization problems were proposed from then on. Ravimohan incorporated CSTRs as an extension to Jackson's effort [8]. Paynter and Haskins used an axial dispersion model to avoid discrete decisions on the reactor types of CSTR and PFR [9]. Ong optimized a serial CSTR network by applying dynamic programming [10]. Achenie and Biegler studied constant dispersion reactors and recycle reactors as network superstructures separately, they also employed macro- and micromixing concepts to bound the performance index defined on a reactor network [11–13]. A superstructure, composed of CSTRs and PFRs approximated by a series of equal sized sub-CSTRs, was presented by Kokossis and Floudas and the resulting mixed-integer nonlinear program (MINLP) was solved using Generalized Benders Decomposition [14,15]. Kokossis and coworkers extended the methodology through the use of stochastic optimization [16,17]. Hillestad presented an optimal control formulation of the reactor design problem, where the resulting two-point boundary value problem was solved by using a steepest descend method [18]. Although superstructure optimization can handle variable density fluid reactors as well, it continues to yield mathematical programming formulations that are nonlinear and nonconvex, and can thus only be solved locally. Furthermore any obtained solutions are only as rich as the initially suggested superstructures.

The Attainable Region (AR) concept was first defined by Horn as the full set of product composition vectors that can be reached by all possible steady-state reactor networks, using only the processes of reaction and mixing/splitting from a given feed point [19]. Gavalas introduced a similar concept that he coined an invariant manifold [1]. The AR concept was further developed by Glasser et al. who employed a geometrically

---

* Corresponding author. Tel.: +1 310 206 0300; fax: +1 310 206 4107.
E-mail address: vasilios@ucla.edu (V.I. Manousiouthakis).

1385-8947/$ – see front matter © 2006 Elsevier B.V. All rights reserved.
doi:10.1016/j.cej.2006.11.004

Nomenclature

C	total molar concentration (kmol/m^3)
C_i	ith component's molar concentration (kmol/m^3)
f	molar flowrate (kmol/s)
f_i	ith component's molar flowrate (kmol/s)
F	volumetric flowrate (m^3/s)
M_i	ith component's molecular weight (kg/kmol)
$\bar{M}$	average molecular weight (kg/kmol)
P	operating pressure (atm)
q	mass flowrate (kg/s)
r_i	ith component's generation rate (kmol/m^3 s)
T	operating temperature (K)
u	input vector of an information map
u_1	extensive variables of input vector of an information map
u_2	intensive/design variables of input vector of an information map
V	reactor volume (m^3)
x_i	ith component's molar fraction
y	output vector of an information map
y_1	extensive variables of output vector of an information map
y_2	intensive/design variables of output vector of an information map
z_i	ith component's mass fraction
Greek letters	
λ	reactor type identifier, 0 for PFR and 1 for CSTR
Φ	input–output information map from u to y representing a process model
Φ_1	component of Φ mapping from u to y_1
Φ_2	component of Φ mapping from u to y_2
σ	reactor design parameter, defined as V/q (m^3 s/kg)
$(\cdot)^{\text{in}}$	property at the inlet of a unit
$(\cdot)^{\text{out}}$	property at the outlet of a unit

based construction [20,21]. Much of their work focuses on geometric interpretations of reaction and mixing and does not employ any assumption on the structure of the reactor network [22–24]. Although AR analysis has been successful in quantifying fundamental limitations of reactor networks, it is only applicable to two- or three-dimensional problems and has only been developed for constant density fluids [13,25–29].

In recent years, research has focused on the computational construction of the AR using linear programming (LP) formulations. The IDEAS framework was first proposed by Wilson and Manousiouthakis [30], and then applied to a wide range of process network synthesis problems [31–35]. IDEAS gives rise to an infinite linear programming (ILP) formulation. The optimal value of this ILP is approximated through solutions of a sequence of finite linear programs of ever increasing size. IDEAS has been applied to the construction of the true AR by Burri et al. [31]. Kauchali et al. also employed an alternative IDEAS formulism to seek the extension of AR candidate sets obtained with traditional geometrically based construction [36]. In doing so, they approximated PFRs with a series of CSTRs. Manousiouthakis et al. also employed a superset guaranteed to contain the true AR [37]. They presented and proved a necessary and sufficient condition for a point in concentration space to belong to the AR, and proposed a so-called Shrink-wrap algorithm for the approximation of the true AR to an arbitrary degree of accuracy, through progressive elimination of extreme grid points not satisfying the above necessary and sufficient condition.

All the aforementioned AR construction works employ the constant density fluid (CDF) assumption. In this work, we present, for the first time, a methodology for the construction of the true AR of reactor networks that consist of variable density fluid (VDF) CSTR and PFR models. This methodology is based on the IDEAS approach to process synthesis. In particular, it is shown that appropriately defined input–output information maps for VDF CSTR/PFR models possess the decomposition and linear input–output properties needed for application of the IDEAS framework. Furthermore, it is established that the IDEAS based Shrink-wrap algorithm is applicable to the VDF AR construction problem when the latter is formulated in mass fraction space. AR construction for three, gas phase, reactor networks with isobaric and isothermal conditions is employed to illustrate the applicability of the IDEAS framework to VDF RNS.

2. The IDEAS approach

2.1. Preliminaries, linearity of the IDEAS framework

The IDEAS framework decomposes the overall process network into two parts: the distribution network (DN) where all possible mixing, splitting, recycling and bypassing of process streams occur; and the process operator (OP) where the action of process unit operations is quantified. Stream information in IDEAS is stored in a way that stream extensive (quantity) properties (e.g. flowrates) and stream intensive (quality) properties (such as concentrations, molar enthalpies, molar fractions, etc.) are dealt with separately. The key development behind IDEAS is that the domain and range of the map quantifying process unit operations in the OP lie in infinite (rather than finite) dimensional spaces. Process operators in traditional representations consider intensive and extensive properties, and design parameters to be variable. In the IDEAS representation, the OP fixes intensive properties and design parameters at any combination of values they can possibly assume. To each of such combination, a vector of extensive variables is assigned, thus giving rise to a sequence, of such extensive variable vectors, belonging to an infinite dimensional space. Furthermore, when the intensive properties and design parameters are fixed, the extensive property input–output map is linear, thus giving rise to a linear OP. In addition, the DN contains solely mixing and splitting operations. Since the intensive properties concerning any stream leaving or entering the DN are known, the resulting balance equations are linear and infinite in number.

The linearity of the OP and DN gives rise to a linear and infinite dimensional feasible region of the IDEAS representation. Consequently, when the objective function is convex, all locally optimal solutions of the resulting process network synthesis problems are guaranteed to be globally optimal.

To elaborate on how the linearity of the OP is achieved, consider a general input/output information map Φ describing a process operation:

$$\Phi : u = \begin{bmatrix} u_1 \\ u_2 \end{bmatrix} \longrightarrow y = \begin{bmatrix} y_1 \\ y_2 \end{bmatrix} = \begin{bmatrix} \Phi_1(u_1, u_2) \\ \Phi_2(u_1, u_2) \end{bmatrix} \tag{1}$$

where $u \in \mathbb{D} = \{u = [\,u_1 \quad u_2\,]^{\mathrm{T}} \in \mathbb{R}^u : \Psi(u_2)u_1 = 0\}$; $y = [\,y_1 \quad y_2\,]^{\mathrm{T}} \in \mathbb{R}^y$; u_1 (u_2) and y_1 (y_2) are extensive (intensive/design) variables of the map's input and output, respectively; $\Psi(u_2)$ is a linear operator for fixed u_2; and Φ_1 and Φ_2 are viewed as components of Φ mapping u to y_1 and y_2, respectively. Usually $\Psi(u_2) = 0$, thus allowing u to be free to move in the whole $\mathbb{R}^u$.

If the following two properties are satisfied by the aforementioned map Φ, then the linearity of the OP of the chemical process under consideration within the IDEAS framework can be achieved:

- 1st property: $y_2 = \Phi_2(u_1, u_2) = \Phi_2(u_2)$, i.e. there is no direct dependence between u_1 and y_2.
- 2nd property: $y_1 = \Phi_1(u_1, u_2) = \Phi_1(u_2)\,u_1$ where $\Phi_1(u_2)$ is a linear map for fixed u_2.

Indeed, properties 1 and 2 ensure that as u_1 varies, y_2 is not affected since it is only a function of u_2, and y_1 is a (possibly u_2 dependent) linear function of u_1. Combined with the definition of $\mathbb{D}$, this implies that if this process operation is part of a network optimization problem in which u_2 is kept fixed, then it gives rise to linear constraints. To take into account all possible values of u_2, the network size is then expanded to include an infinite number of possible unit operations each of which corresponds to a possible value of u_2. Consequently, the OP can be modelled by an infinite number of units, each of which has prior specified values of $u_2 = \bar{u}_2$, which in return specifies $y_2 = \bar{y}_2$ from $y_2 = \Phi_2(u_2)$, and generates linear constraints $y_1 = \Phi_1(\bar{u}_2)\,u_1$, $\Psi(\bar{u}_2)\,u_1 = 0$.

To demonstrate, consider a constant density fluid CSTR in which a 2nd order reaction: $2A_1 \rightarrow A_2$, is carried out with reaction rate coefficient k. The associated model is

$$C_1^{\mathrm{out}} - C_1^{\mathrm{in}} = -2\tau k (C_1^{\mathrm{out}})^2 \tag{2}$$

$$C_2^{\mathrm{out}} - C_2^{\mathrm{in}} = \tau k (C_1^{\mathrm{out}})^2 \tag{3}$$

$$V = \tau F \tag{4}$$

where F is the volumetric flowrate in and out of the reactor (m^3/s); C_1^{in} (C_1^{out}) and C_2^{in} (C_2^{out}) are the molar concentrations of A_1 and A_2 at the reactor inlet (outlet), respectively ($\mathrm{kmol/m}^3$); V the reactor volume (m^3); and τ is the reactor residence time (s).

The linearity of the OP can be attained in a number of ways. First, Φ, u and y can be defined as

$$\Phi : u \rightarrow y, \quad u = \begin{bmatrix} u_1 \\ \text{– –} \\ u_2 \end{bmatrix} = \begin{bmatrix} F \\ \text{– –} \\ C_1^{\mathrm{in}} \\ C_2^{\mathrm{in}} \\ \tau \end{bmatrix};$$

$$y = \begin{bmatrix} y_1 \\ \text{– –} \\ y_2 \end{bmatrix} = \begin{bmatrix} F \\ V \\ \text{– –} \\ C_1^{\mathrm{out}} \\ C_2^{\mathrm{out}} \end{bmatrix}$$

where $u \in \mathbb{R}^4$, $\Psi(u_2) = 0$, $y \in \mathbb{R}^4$. It is easy to prove that Φ possesses the aforementioned two properties needed for OP linearity. Indeed,

$$\Phi_2 : u_2 \overset{(2)(3)}{\rightarrow} y_2 = \Phi_2(u_2) = \begin{bmatrix} \dfrac{-1 + \sqrt{1 + 8\tau k C_1^{\mathrm{in}}}}{4\,\tau k} \\ C_2^{\mathrm{in}} + \tau k \left(\dfrac{-1 + \sqrt{1 + 8\tau k C_1^{\mathrm{in}}}}{4\tau k} \right)^2 \end{bmatrix}$$

and thus Φ_2 satisfies property 1. Furthermore,

$$\Phi_1(u_2) \triangleq \begin{bmatrix} 1 & \tau \end{bmatrix}^{\mathrm{T}} : u_1 \overset{(4)}{\rightarrow} y_1$$

is a linear operator for any fixed u_2, thus satisfying property 2.

Another way Φ, u and y can be defined is as follows:

$$\Phi : u \rightarrow y, \quad u = \begin{bmatrix} u_1 \\ \text{– –} \\ u_2 \end{bmatrix} = \begin{bmatrix} F \\ \text{– –} \\ C_1^{\mathrm{out}} \\ C_2^{\mathrm{out}} \\ C_1^{\mathrm{in}} \end{bmatrix};$$

$$y = \begin{bmatrix} y_1 \\ \text{– –} \\ y_2 \end{bmatrix} = \begin{bmatrix} F \\ V \\ \text{– –} \\ C_2^{\mathrm{in}} \\ \tau \end{bmatrix}$$

where $u \in \mathbb{R}^4$, $\Psi(u_2) = 0$, $y \in \mathbb{R}^4$. Thus

$$\Phi_2 : u_2 \overset{(2)(3)}{\rightarrow} y_2 = \Phi_2(u_2) = \begin{bmatrix} C_2^{\mathrm{out}} - \dfrac{1}{2}(C_1^{\mathrm{in}} - C_1^{\mathrm{out}}) \\ \dfrac{C_1^{\mathrm{in}} - C_1^{\mathrm{out}}}{2k(C_1^{\mathrm{out}})^2} \end{bmatrix};$$

$$\Phi_1(u_2) \triangleq \begin{bmatrix} 1 \ \tau \end{bmatrix}^{\mathrm{T}} = \begin{bmatrix} 1 & \dfrac{C_1^{\mathrm{in}} - C_1^{\mathrm{out}}}{2k(C_1^{\mathrm{out}})^2} \end{bmatrix}^{\mathrm{T}} : u_1 \overset{(4)}{\rightarrow} y_1$$

Φ_2 satisfies property 1, and for any fixed u_2, τ is fixed, which ensures $\Phi_1(u_2)$ is a linear operator, thus satisfying property 2.

Finally, another way Φ, u and y can be defined is by first rewriting the CSTR model as

$$FC_1^{\text{out}} - f_1^{\text{in}} = -2Vk(C_1^{\text{out}})^2 \tag{5}$$

$$FC_2^{\text{out}} - f_2^{\text{in}} = Vk(C_1^{\text{out}})^2 \tag{6}$$

where f_1^{in} and f_2^{in} are the inlet molar flowrates of A_1 and A_2, respectively (kmol/s). Then,

$$\Phi : u \to y, \quad u = \begin{bmatrix} u_1 \\ -- \\ u_2 \end{bmatrix} = \begin{bmatrix} f_1^{\text{in}} \\ f_2^{\text{in}} \\ F \\ V \\ -- \\ C_1^{\text{out}} \\ C_2^{\text{out}} \end{bmatrix}; \qquad y = [y_1] = [F]$$

where $u \in \mathbb{D} = \{u \in \mathbb{R}^6 : \Psi(u_2)u_1 = 0\}$; $y = y_1 \in \mathbb{R}^1$;

$$\Psi(u_2) = \begin{bmatrix} -1 & 0 & C_1^{\text{out}} & 2k(C_1^{\text{out}})^2 \\ 0 & -1 & C_2^{\text{out}} & -k(C_1^{\text{out}})^2 \end{bmatrix}$$

As a result, property 1 is automatically satisfied since there is no need to define a Φ_2. Similarly, property 2 is satisfied since the map $\Phi_1(u_2) \triangleq \begin{bmatrix} 0 & 0 & 1 & 0 \end{bmatrix} : u_1 \to y_1$ is linear.

Different ways of attaining linearity of the OP will result in different IDEAS optimization formulations with different computational characteristics.

2.2. Unit operation models for variable density fluid reactors

In this section, it is shown that the two properties, shown in Section 2.1 to lead to OP linearity, are satisfied by steady state, isobaric, isothermal, VDF CSTR and PFR models.

2.2.1. Variable density fluid CSTR models

Molar model. Consider a VDF CSTR containing n components whose generation rates are expressed in molar concentrations. A typical model for this unit operation is expressed in terms of molar flowrates and molar fractions as follows:

$$f^{\text{out}}x_i^{\text{out}} - f^{\text{in}}x_i^{\text{in}} = Vr_i(\{C_k^{\text{out}}\}_{k=1}^n), \quad \forall i = 1, \ldots, n-1 \tag{7}$$

$$f^{\text{out}} - f^{\text{in}} = V\sum_{i=1}^{n} r_i(\{C_k^{\text{out}}\}_{k=1}^n) \tag{8}$$

$$C_k^{\text{out}} = C_k^{\text{out}}(\{x_j^{\text{out}}\}_{j=1}^{n-1}, T, P), \quad \forall k = 1, \ldots, n \tag{9}$$

where f^{in} and f^{out} are the molar flowrates at the reactor inlet and outlet, respectively; x_i^{in} and x_i^{out} are the ith component's molar fractions at the reactor inlet and outlet, respectively; and r_i is the ith component's molar generation rate per unit volume. Eqs. (7) and (8) are component and total balances, while Eq. (9) says that each component concentration is a function of temperature, pressure and molar fractions. Chemical thermodynamics provides several models that can be brought in the form of Eq. (9) for both gas and liquid phase mixtures. For example, if a compressibility factor ($\mathcal{Z}$) model is used, one could write $C_k = x_k(P/RT)(1/\mathcal{Z})$, where R is the gas constant; $\mathcal{Z}$ is a function of $\{x_j\}_{j=1}^{n-1}$, T, P. In the simplest example of an ideal gas phase mixture, we then have $\mathcal{Z} = 1$.

By defining two parameters: $\zeta = V/f^{\text{in}}$; $\eta = f^{\text{out}}/f^{\text{in}}$, the model can be rewritten as

$$\eta x_i^{\text{out}} - x_i^{\text{in}} = \zeta r_i(\{C_k^{\text{out}}\}_{k=1}^n), \quad \forall i = 1, \ldots, n-1 \tag{10}$$

$$\eta - 1 = \zeta\sum_{i=1}^{n} r_i(\{C_k^{\text{out}}\}_{k=1}^n) \tag{11}$$

$$C_k^{\text{out}} = C_k^{\text{out}}(\{x_j^{\text{out}}\}_{j=1}^{n-1}, T, P), \quad \forall k = 1, \ldots, n \tag{12}$$

$$f^{\text{out}} = \eta f^{\text{in}} \tag{13}$$

$$V = \zeta f^{\text{in}} \tag{14}$$

The above equations can be used to define an input–output information map $\Phi : u \to y$ as follows:

$$u = \begin{bmatrix} u_1 \\ -- \\ u_2 \end{bmatrix} = \begin{bmatrix} f^{\text{in}} \\ -- \\ x_1^{\text{in}} \\ x_2^{\text{in}} \\ \vdots \\ x_{n-1}^{\text{in}} \\ \zeta \\ T \\ P \end{bmatrix}; \qquad y = \begin{bmatrix} y_1 \\ -- \\ y_2 \end{bmatrix} = \begin{bmatrix} f^{\text{out}} \\ V \\ -- \\ x_1^{\text{out}} \\ x_2^{\text{out}} \\ \vdots \\ x_{n-1}^{\text{out}} \\ \eta \end{bmatrix} \tag{15}$$

$u \in \mathbb{R}^{n+3}$, $\Psi(u_2) = 0$, $y \in \mathbb{R}^{n+2}$.

The aforementioned map satisfies properties 1 and 2 outlined earlier and therefore the IDEAS approach is applicable to this VDF CSTR model. Indeed, Φ_2 and $\Phi_1(u_2)$ take the form:

$$\Phi_2 : u_2 \xrightarrow{(10),(11),(12)} y_2;$$

$$\Phi_1(u_2) \triangleq \begin{bmatrix} \eta(u_2) & \zeta \end{bmatrix}^{\text{T}} : u_1 \xrightarrow{(13),(14)} y_1$$

Once again, when u_2 is fixed, $\eta(u_2)$ is fixed and Φ_1 becomes a linear operator.

Mass model. Taking into account the fact that no matter what reactions happen in a reactor, the total mass flowrate q will not change because of the mass conservation principle (i.e. $q^{\text{in}} = q^{\text{out}} = q$), an alternative VDF CSTR model can be developed in terms of mass flowrates and mass fractions as follows:

$$qz_i^{\text{out}} - qz_i^{\text{in}} = VM_i r_i(\{C_k^{\text{out}}\}_{k=1}^n), \quad \forall i = 1, \ldots, n-1 \tag{16}$$

$$C_k^{\text{out}} = C_k^{\text{out}}(\{z_j^{\text{out}}\}_{j=1}^{n-1}, T, P), \quad \forall k = 1, \ldots, n \tag{17}$$

where z_i^{in} and z_i^{out} are the ith component's mass fractions at the reactor inlet and outlet, respectively; and M_i is the ith component's molecular weight. Recall the following relation for a mixture:

$$\bar{M} = \sum_{j=1}^{n} x_j M_j = \frac{1}{\sum_{j=1}^{n}(z_j/M_j)}; \qquad x_i = z_{\mathrm{i}} \frac{\bar{M}}{M_i} \tag{18}$$

where $\bar{M}$ is the average molecular weight. Thus, Eq. (17) can be obtained by combining Eqs. (9) and (18). Then by defining the design parameter $\sigma = V/q$, the model becomes:

$$z_i^{\mathrm{out}} - z_i^{\mathrm{in}} = \sigma M_i r_i(\{C_k^{\mathrm{out}}\}_{k=1}^{n}), \quad \forall i = 1, \ldots, n-1 \tag{19}$$

$$C_k^{\mathrm{out}} = C_k^{\mathrm{out}}(\{z_j^{\mathrm{out}}\}_{j=1}^{n-1}, T, P), \quad \forall k = 1, \ldots, n \tag{20}$$

$$V = \sigma q \tag{21}$$

An input–output information map $\Phi : u \to y$ can then be defined as

$$u = \begin{bmatrix} u_1 \\ -- \\ u_2 \end{bmatrix} = \begin{bmatrix} q \\ -- \\ z_1^{\mathrm{in}} \\ z_2^{\mathrm{in}} \\ \vdots \\ z_{n-1}^{\mathrm{in}} \\ \sigma \\ T \\ P \end{bmatrix}; \qquad y = \begin{bmatrix} y_1 \\ -- \\ y_2 \end{bmatrix} = \begin{bmatrix} q \\ V \\ -- \\ z_1^{\mathrm{out}} \\ z_2^{\mathrm{out}} \\ \vdots \\ z_{n-1}^{\mathrm{out}} \end{bmatrix} \tag{22}$$

where $u \in \mathbb{R}^{n+3}$, $\Psi(u_2) = 0$, $y \in \mathbb{R}^{n+1}$. Φ_2 and $\Phi_1(u_2)$ become:

$$\Phi_2 : u_2 \overset{(19),(20)}{\rightarrow} y_2; \qquad \Phi_1(u_2) \triangleq \begin{bmatrix} 1 & \sigma \end{bmatrix}^{\mathrm{T}} : u_1 \overset{(21)}{\rightarrow} y_1$$

2.2.2. Variable density fluid PFR models

Different from CSTR models which include a set of nonlinear algebraic equations, PFR models consist of a set of ordinary differential equations. As a result, besides defining parameters similarly to CSTR models, corresponding differential elements need to be defined as well.

Molar model. For the molar flowrate/fraction PFR model, $\bar{\zeta} = v/f^{\mathrm{in}}$ and $\bar{\eta} = f/f^{\mathrm{in}}$ are defined such that the differential element $\mathrm{d}(fx_i)/\mathrm{d}v$ becomes $\mathrm{d}(\bar{\eta}x_i)\mathrm{d}\bar{\zeta}$. Thus the model can be written as

$$\frac{\mathrm{d}(\bar{\eta}x_i)}{\mathrm{d}\bar{\zeta}} = r_i(\{C_k\}_{k=1}^{n}), \quad \forall i = 1, \ldots, n-1 \tag{23}$$

$$\frac{\mathrm{d}\bar{\eta}}{\mathrm{d}\bar{\zeta}} = \sum_{i=1}^{n} r_i(\{C_k\}_{k=1}^{n}) \tag{24}$$

$$C_k = C_k(\{x_j\}_{j=1}^{n-1}, T, P), \quad \forall k = 1, \ldots, n \tag{25}$$

$$\bar{\zeta} = 0 \Rightarrow \bar{\eta} = 1; \quad x_i = x_i^{\mathrm{in}}, \quad \forall i = 1, \ldots, n-1 \tag{26}$$

$$\bar{\zeta} = \zeta \Rightarrow \bar{\eta} = \eta; \quad x_i = x_i^{\mathrm{out}}, \quad \forall i = 1, \ldots, n-1 \tag{27}$$

$$f^{\mathrm{out}} = \eta f^{\mathrm{in}} \tag{28}$$

$$V = \zeta f^{\mathrm{in}} \tag{29}$$

To depict an input–output information map $\Phi : u \to y$ for IDEAS, u and y can be defined the same way as Eq. (15), and Φ_2 and $\Phi_1(u_2)$ take the form:

$$\Phi_2 : u_2 \overset{(23),(24),(25),(26),(27)}{\rightarrow} y_2;$$

$$\Phi_1(u_2) \triangleq \begin{bmatrix} \eta(u_2) & \zeta \end{bmatrix}^{\mathrm{T}} : u_1 \overset{(28),(29)}{\rightarrow} y_1$$

Mass model. For the mass flowrate/fraction PFR model, $\bar{\sigma} = v/q$ is defined such that the differential element $\mathrm{d}(qz_i)/\mathrm{d}v$ becomes $\mathrm{d}z_i/\mathrm{d}\bar{\sigma}$. The model can then be written as

$$\frac{\mathrm{d}z_i}{\mathrm{d}\bar{\sigma}} = M_i r_i(\{C_k\}_{k=1}^{n}), \quad \forall i = 1, \ldots, n-1 \tag{30}$$

$$C_k = C_k(\{z_j\}_{j=1}^{n-1}, T, P), \quad \forall k = 1, \ldots, n \tag{31}$$

$$\bar{\sigma} = 0 \Rightarrow z_i = z_i^{\mathrm{in}}, \quad \forall i = 1, \ldots, n-1 \tag{32}$$

$$\bar{\sigma} = \sigma \Rightarrow z_i = z_i^{\mathrm{out}}, \quad \forall i = 1, \ldots, n-1 \tag{33}$$

$$V = \sigma q \tag{34}$$

u and y can be defined the same way as Eq. (22), and Φ_2 and $\Phi_1(u_2)$ become:

$$\Phi_2 : u_2 \overset{(30),(31),(32),(33)}{\rightarrow} y_2; \qquad \Phi_1(u_2) \triangleq \begin{bmatrix} 1 & \sigma \end{bmatrix}^{\mathrm{T}} : u_1 \overset{(34)}{\rightarrow} y_1$$

The above verifies the claim that properties leading to OP linearity are satisfied by steady state, isobaric, isothermal, VDF CSTR and PFR models. Whether the molar or mass based models are employed is the designer's choice. For example, when reaction rates are described in terms of partial pressures, the molar flowrate/fraction models may be preferable. In this work, the mass flowrate/fraction models for both VDF CSTRs and PFRs are used.

It is worth pointing out here that the above models are general and thus suitable for handling the situation where the constant density assumption is employed as well. For example, consider the CDF CSTR model:

$$C_i^{\mathrm{out}} - C_i^{\mathrm{in}} = \frac{V}{F^{\mathrm{in}}} r_i(\{C_k\}_{k=1}^{n}), \quad \forall i = 1, \ldots, n \tag{35}$$

and let F^{in} (F^{out}), ρ^{in} (ρ^{out}) be volumetric flowrate and mass density at reactor inlet (outlet), respectively. Then, by multiplying M_i/ρ^{in} on both sides, and taking into account that: $F^{\mathrm{in}}\rho^{\mathrm{in}} = F^{\mathrm{out}}\rho^{\mathrm{out}} = g$; $C_i^{\mathrm{out}} M_i/\rho^{\mathrm{in}} = \rho^{\mathrm{out}} z_i^{\mathrm{out}}/\rho^{\mathrm{in}} = z_i^{\mathrm{out}}$ and $C_i^{\mathrm{in}} M_i/\rho^{\mathrm{in}} = z_i^{\mathrm{in}}$, one gets

$$z_i^{\mathrm{out}} - z_i^{\mathrm{in}} = \frac{V}{g^{\mathrm{in}}} M_i r_i(\{C_k\}_{k=1}^{n}), \quad \forall i = 1, \ldots, n \tag{36}$$

which is Eq. (19).

2.3. IDEAS representation for VDF RNS

2.3.1. Variable definitions

Fig. 1 illustrates the IDEAS representation for VDF reactor networks with $\mathbf{N}_{\mathrm{I}}$ external (network) inlet streams and $\mathbf{N}_{\mathrm{O}}$ external (network) outlet streams.

Each network inlet stream is represented by $q^{\mathrm{I}}(j)$ and $z^{\mathrm{I}}(j)\,\forall j = 1, \ldots, N_{\mathrm{I}}$, where the scalar $q^{\mathrm{I}}(j)$ represents the extensive property (mass flowrate) of the jth network inlet stream and the vector $z^{\mathrm{I}}(j)$ represents the intensive properties (mass fractions) of the jth network inlet stream defined as

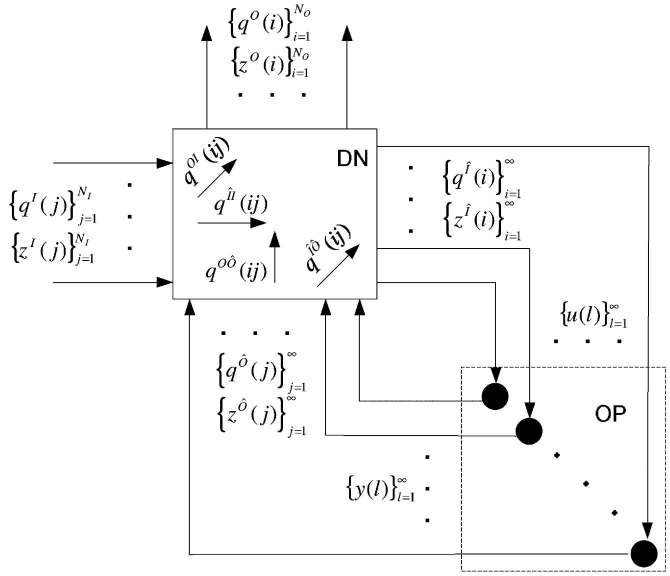

Fig. 1. IDEAS representation for process networks.

$z^{\mathrm{I}}(j) = \left[z_1^{\mathrm{I}}(j) \quad z_2^{\mathrm{I}}(j) \quad \cdots \quad z_{n-1}^{\mathrm{I}}(j) \right]^{\mathrm{T}}$. The sequence of network inlet stream extensive and intensive properties are defined as q^{I} and z^{I}:

$$q^{\mathrm{I}} = \{q^{\mathrm{I}}(1), q^{\mathrm{I}}(2), \ldots, q^{\mathrm{I}}(N_{\mathrm{I}})\};$$

$$z^{I} = \{z^{\mathrm{I}}(1), z^{\mathrm{I}}(2), \ldots, z^{\mathrm{I}}(N_{\mathrm{I}})\}$$

Similarly, the following property sequences are defined: q^{O} and z^{O} for the network outlet; $q^{\hat{\mathrm{I}}}$ and $z^{\hat{\mathrm{I}}}$ for the OP inlet; $q^{\hat{\mathrm{O}}}$ and $z^{\hat{\mathrm{O}}}$ for the OP outlet and four sets of cross-flow streams each of which is represented by a flowrate with destination and origin: q^{OI}, $q^{\hat{\mathrm{I}}\mathrm{I}}$, $q^{\mathrm{O}\hat{\mathrm{O}}}$, $q^{\hat{\mathrm{I}}\hat{\mathrm{O}}}$ are defined as well (Table 1). Each process unit in the OP is represented by a map $\Phi(l) : u(l) \to y(l) \forall l = 1, \ldots, \infty$.

2.3.2. Optimization formulation

Under the steady-state, isobaric and isothermal assumptions, the IDEAS optimization formulation for VDF RNS can then be written as

$$\nu = \inf_{(q^{\mathrm{I}}, q^{\mathrm{O}}, q^{\hat{\mathrm{I}}}, q^{\hat{\mathrm{O}}}, q^{\mathrm{OI}}, q^{\hat{\mathrm{I}}\mathrm{I}}, q^{\mathrm{O}\hat{\mathrm{O}}}, q^{\hat{\mathrm{I}}\hat{\mathrm{O}}})} \mathrm{OBJ} \tag{37}$$

s.t.

$$q^{\mathrm{I}}(j) = \sum_{i=1}^{N_{\mathrm{O}}} q^{\mathrm{OI}}(i, j) + \sum_{i=1}^{\infty} q^{\hat{\mathrm{I}}\mathrm{I}}(i, j), \quad \forall j = 1, \ldots, N_{\mathrm{I}} \tag{38}$$

$$q^{\mathrm{O}}(i) = \sum_{j=1}^{N_{\mathrm{I}}} q^{\mathrm{OI}}(i, j) + \sum_{j=1}^{\infty} q^{\mathrm{O}\hat{\mathrm{O}}}(i, j), \quad \forall i = 1, \ldots, N_{\mathrm{O}} \tag{39}$$

$$q^{\hat{\mathrm{I}}}(i) = \sum_{j=1}^{N_{\mathrm{I}}} q^{\hat{\mathrm{I}}\mathrm{I}}(i, j) + \sum_{j=1}^{\infty} q^{\hat{\mathrm{I}}\hat{\mathrm{O}}}(i, j), \quad \forall i = 1, \ldots, \infty \tag{40}$$

$$q^{\hat{\mathrm{O}}}(j) = \sum_{i=1}^{N_{\mathrm{O}}} q^{\mathrm{O}\hat{\mathrm{O}}}(i, j) + \sum_{i=1}^{\infty} q^{\hat{\mathrm{I}}\hat{\mathrm{O}}}(i, j), \quad \forall j = 1, \ldots, \infty \tag{41}$$

Table 1
Variable and parameter definitions

N_{I}	Number of network(external) inlet streams
N_{O}	Number of network(external) outlet streams
$z_k^{\mathrm{I}}(j)$	kth component mass fraction in the jth network inlet $k = 1, n-1; j = 1, N_{\mathrm{I}}$
$z_k^{\mathrm{O}}(i)$	kth component mass fraction in the ith network outlet $k = 1, n-1; i = 1, N_{\mathrm{O}}$
$z_k^{\hat{\mathrm{I}}}(i)$	kth component mass fraction in the ith OP inlet $k = 1, n-1; i = 1, \infty$
$z_k^{\hat{\mathrm{O}}}(j)$	kth component mass fraction in the jth OP outlet $k = 1, n-1; j = 1, \infty$
$q^{\mathrm{I}}(j)$	jth network inlet mass flowrate $j = 1, N_{\mathrm{I}}$
$q^{\mathrm{O}}(i)$	ith network outlet mass flowrate $i = 1, N_{\mathrm{O}}$
$q^{\hat{\mathrm{I}}}(i)$	ith OP (reactor) inlet mass flowrate $i = 1, \infty$
$q^{\hat{\mathrm{O}}}(j)$	jth OP (reactor) outlet mass flowrate $i = 1, \infty$
$q^{\mathrm{OI}}(ij)$	Flowrate from the jth network inlet to the ith network outlet $i = 1, N_{\mathrm{O}}; j = 1, N_{\mathrm{I}}$
$q^{\hat{\mathrm{I}}\mathrm{I}}(ij)$	Flowrate from the jth network inlet to the ith OP inlet $i = 1, \infty; j = 1, N_{\mathrm{I}}$
$q^{\mathrm{O}\hat{\mathrm{O}}}(ij)$	Flowrate from the jth OP outlet to the ith network outlet $i = 1, N_{\mathrm{O}}; j = 1, \infty$
$q^{\hat{\mathrm{I}}\hat{\mathrm{O}}}(ij)$	Flowrate from the jth OP outlet to the ith OP inlet $i = 1, \infty; j = 1, \infty$
$u(l)$	Input of the information map for the lth process unit $l = 1, \infty$
$y(l)$	Output of the information map for the lth process unit $l = 1, \infty$

$$z_k^{\hat{\mathrm{I}}}(i) q^{\hat{\mathrm{I}}}(i) = \sum_{j=1}^{N_{\mathrm{I}}} z_k^{\mathrm{I}}(j) q^{\hat{\mathrm{I}}\mathrm{I}}(i, j) + \sum_{j=1}^{\infty} z_k^{\hat{\mathrm{O}}}(j) q^{\hat{\mathrm{I}}\hat{\mathrm{O}}}(i, j),$$
$$\forall k = 1, \ldots, n-1; \forall i = 1, \ldots, \infty \tag{42}$$

$$(q^{\mathrm{O}}(i))^{\mathrm{low}} \le q^{\mathrm{O}}(i) \le (q^{\mathrm{O}}(i))^{\mathrm{upp}}, \quad \forall i = 1, \ldots, N_{\mathrm{O}} \tag{43}$$

$$\begin{aligned}(z_k^{\mathrm{O}}(i))^{\mathrm{low}} q^{\mathrm{O}}(i) &\le \sum_{j=1}^{N_{\mathrm{I}}} z_k^{\mathrm{I}}(j) q^{\mathrm{OI}}(i, j) + \sum_{j=1}^{\infty} z_k^{\hat{\mathrm{O}}}(j)\, q^{\mathrm{O}\hat{\mathrm{O}}}(i, j) \\ &\le (z^{\mathrm{O}}(i))^{\mathrm{upp}} q^{\mathrm{O}}(i), \quad \forall k = 1, \ldots, n-1; \\ &\quad \forall i = 1, \ldots, N_{\mathrm{O}}\end{aligned} \tag{44}$$

$$q^{\hat{\mathrm{O}}}(i) = q^{\hat{\mathrm{I}}}(i), \quad \forall i = 1, \ldots, \infty \tag{45}$$

$$\begin{aligned}&q^{\mathrm{I}} \ge 0; \quad q^{\mathrm{O}} \ge 0; \quad ; q^{\hat{\mathrm{I}}} \ge 0; \quad q^{\hat{\mathrm{O}}} \ge 0; \\ &q^{\mathrm{OI}} \ge 0; \quad q^{\hat{\mathrm{I}}\mathrm{I}} \ge 0; \quad q^{\mathrm{O}\hat{\mathrm{O}}} \ge 0; \quad q^{\hat{\mathrm{I}}\hat{\mathrm{O}}} \ge 0\end{aligned} \tag{46}$$

where sequences $(z^{\mathrm{O}})^{\mathrm{low}}$ $((z^{\mathrm{O}})^{\mathrm{upp}})$ and $(q^{\mathrm{O}})^{\mathrm{low}}$ $((q^{\mathrm{O}})^{\mathrm{upp}})$ are lower (upper) bounds of sequences z^{O} and q^{O}, respectively. Eqs. (38)–(41) correspond to total mass balances in the DN; Eqs. (42) and (44) represent component balances in the DN. In this work, the linearity of the OP is achieved by defining $\Phi : u \to y$ as follows:

$$u(l)=\begin{bmatrix} u_1(l) \\ -- \\ u_2(l) \end{bmatrix}=\begin{bmatrix} q^{\hat{\mathrm{I}}}(l) \\ -- \\ z_1^{\hat{\mathrm{I}}}(l) \\ z_2^{\hat{\mathrm{I}}}(l) \\ \vdots \\ z_{n-1}^{\hat{\mathrm{I}}}(l) \\ \sigma(l) \\ \lambda(l) \end{bmatrix};$$

$$y(l)=\begin{bmatrix} y_1(l) \\ -- \\ y_2(l) \end{bmatrix}=\begin{bmatrix} q^{\hat{\mathrm{O}}}(l) \\ V(l) \\ -- \\ z_1^{\hat{\mathrm{O}}}(l) \\ z_2^{\hat{\mathrm{O}}}(l) \\ \vdots \\ z_{n-1}^{\hat{\mathrm{O}}}(l) \end{bmatrix}, \quad \forall l=1,\ldots,\infty \tag{47}$$

where $u(l)\in\mathbb{R}^{n+2}$, $\Psi(u_2(l))=0$, λ is allowed only to be 0 or 1 and is used as a technology flag to identify the reactor type (i.e. 0 for PFR and 1 for CSTR), $y\in\mathbb{R}^{n+1}$. Correspondingly, $\Phi_2(l): u_2(l)\rightarrow y_2(l)$ becomes

$$\frac{\mathrm{d}z_k}{\mathrm{d}\bar{\sigma}}=M_k r_k(\{z_j\}_{j=1}^{n-1}, T, P), \quad \forall k=1,\ldots,n-1;$$

$$z_k|_{\bar{\sigma}=0}=z_k^{\hat{\mathrm{I}}}(l), \quad z_k|_{\bar{\sigma}=\sigma(l)}=z_k^{\hat{\mathrm{O}}}(l), \quad \forall k=1,\ldots,n-1$$

$$\text{if } \lambda(l)=0 \tag{48}$$

$$z_k^{\hat{\mathrm{O}}}(l)-z_k^{\hat{\mathrm{I}}}(l)=\sigma(l)M_k r_k(\{z_j^{\hat{\mathrm{O}}}(l)\}_{j=1}^{n-1}, T, P),$$
$$\forall k=1,\ldots,n-1, \quad \text{if } \lambda(l)=1 \tag{49}$$

and $\Phi_1(l): u_1(l)\rightarrow y_1(l)$ takes the form: $[\,1\ \sigma(l)\,]^{\mathrm{T}}$. The process is elaborated as the following: by fixing u_2 at any possible condition, and by calculating y_2 as $\Phi_2(u_2)$, one then creates a linear OP that maps an infinite number of variables u_1 through the linear map $\Phi_1(u_2)$ to an infinite number of variables y_1. This linear OP is represented by Eq. (45), since reactor volumes $\{V(l)\}_{l=1}^{\infty}$ do not show up in the constrains and can be substituted by $V(l)=\sigma(l)q(l)$ if they are in the OBJ. It is worth pointing out that components of sequence $z^{\hat{\mathrm{I}}}$ could be identical, and so does $z^{\hat{\mathrm{O}}}$. Indeed, it is easy to find out that there could be up to infinite number of same mass fraction vector as σ varies from 0 to ∞.

A convex (linear) functional is considered as an objective for the IDEAS optimization. A variety of objectives can be realized by appropriate selection of the cost coefficients, including maximization of concentration, yield, selectivity or economic considerations such as minimization of total reactor volume.

3. VDF AR construction

The VDF RNS AR problem can be stated as follows: given reaction kinetic information, what is the set of points in composition (molar concentration, molar fraction or mass fraction) space that can be attained as product compositions of a VDF reactor network with a given feed.

3.1. IDEAS adaptation to VDF AR construction

Considering an isobaric, isothermal reactor network with a single inlet and a single outlet (i.e. $\mathbf{N_I}=\mathbf{N_O}=1$), a point on the AR boundary can be found by formulating an objective function that maximizes the mass fraction of the desired product (i.e. $\tilde{k}$th component) in the network outlet stream, while fixing the mass fractions of concerned component(s) (i.e. use $\tilde{K}$ to represent the union of the indices of these components) in the outlet stream at their coordinates' value(s). Apparently $\tilde{k}\not\in\tilde{K}\subset\{i\}_{i=1}^{n}$. Then the total AR boundary can be constructed in this pointwise manner. The objective function is formulated as

$$\mathrm{OBJ}=z_{\tilde{k}}^{\mathrm{O}}(1) \tag{50}$$

In addition, the lower/upper bounds $(z^{\mathrm{O}}(1))^{\mathrm{low}}$, $(z^{\mathrm{O}}(1))^{\mathrm{upp}}$ are selected to be

$$(z_k^{\mathrm{O}}(1))^{\mathrm{low}}=(z_k^{\mathrm{O}}(1))^{\mathrm{upp}}=\widetilde{z_k^{\mathrm{O}}(1)}, \quad \forall k\in\tilde{K} \tag{51}$$

where $\widetilde{z_k^{\mathrm{O}}(1)}$ is the fixed value of $z_k^{\mathrm{O}}(1)$ in the network outlet.

The aforementioned IDEAS optimization formulation is an infinite dimensional linear program, whose solution can be approximated by the optimal solutions of a series of finite linear programs of increasing size. There are plenty of ways to generate finite dimensional programs. To show how this is done, consider the CSTR example of Section 2.1 and the second way of achieving linearity of the OP. At the outset, we presume that we know lower/upper bounds of C_1^{out}, C_2^{out}, C_1^{in}. These bounds may be crude, or may be derived from brief analysis of the kinetics. By introducing a uniform grid in all three dimensions (C_1^{out}, C_2^{out}, C_1^{in}) and using Eqs. (2) and (3) to calculate C_2^{in}, τ, we can generate a finite number of feasible CSTRs and corresponding OP inlet/outlet streams.

3.2. Applicability of the Shrink-wrap algorithm for VDF AR construction

The IDEAS formulation for reactor network synthesis of variable density flow in terms of mass flowrates and component mass fractions (Eqs. (37)–(46)) is analogous to that formulated by Manousiouthakis et al. for constant density reactor network synthesis, in terms of volumetric flowrates and component molar concentrations [37]. Indeed, using the definitions of (in)active reactors, isolated subnetworks and well-connected networks/subnetworks, and following the analysis in Ref. [37] by replacing volumetric flowrates and component molar concentrations with mass flowrates and component mass fractions, respectively, one can readily obtain a similar theorem as Theorem 2 in Ref. [37], which is restated as follows.

Theorem 1. *A necessary and sufficient condition for a point in mass fraction space to be in the VDF AR is that it must belong to the convex hull, defined by the feed point mass fraction vector and those outlet mass fraction vectors corresponding to active reactors that do not belong to an isolated reactor subnetwork, and whose inlet mass fraction vectors are also in the convex hull.*

As a result, the Shrink-wrap algorithm is applicable to VDF AR construction problems. This is a significant development which allows identification of the VDF AR without solution of large finite linear programs. It is important to emphasize at this point that extension of the Shrink-wrap algorithm to the VDF AR construction problem is not possible for mole based reactor models. As discussed earlier, mass flowrate/fraction and molar flowrate/fraction models are possible for VDF CSTR's and PFR's. Both are eligible to be employed in the IDEAS framework for reactor network synthesis, and lead to infinite linear programming formulations. However, since the molar flowrate through a VDF reactor changes, Eq. (45) is altered as follows:

$$f^{\hat{\mathrm{O}}}(i) = \eta(i) f^{\hat{\mathrm{I}}}(i), \quad \forall\, i = 1, \ldots, \infty \tag{52}$$

Because of this change, the analysis in Ref. [37] cannot be carried through when replacing volumetric flowrates and component molar concentrations with molar flowrates and component molar fractions, respectively. Fortunately, however the use of mass flowrates/fractions permits the use of the Shrink-wrap algorithm in quantifying the VDF AR.

3.3. Reactor network for desired product composition

In the ILP optimization methodology, identification of each AR boundary point is carried out simultaneously with the identification of the reactor network that delivers this point as its exit. The composition of AR interior points can then be reached through mixing of boundary points with the feed. However for the Shrink-wrap algorithm, these reactor networks are not identified as the AR is constructed (Shrunk) from a superset. Nevertheless, once the AR is identified, a reactor network can be identified that delivers any point in the AR as its exit.

Let the CSTR (PFR) forward trajectories from the feed be denoted as $T_1(\check{T}_1)$, and the convex hull defined by T_1 and $\check{T}_1$ be denoted as H_1 (a closed hull). In addition, consider a desired product composition point in the AR, and let the CSTR (PFR) backward trajectories from this point, excluding the point itself, be denoted as $T_2(\check{T}_2)$. Let also the convex hull defined by H_1 and the desired composition point be denoted as H_2 (a closed hull). If the desired composition point belongs to $T_1(\check{T}_1)$, then a CSTR (PFR) from the feed can be used to deliver the desired composition as its exit. If the desired composition point does not belong to T_1 and $\check{T}_1$, but belongs to H_1, then a reactor network, consisting of one or two reactors (a CSTR and/or a PFR from the feed), can be used; the desired composition can be obtained through mixing of the feed and product(s) of the reactor(s). If the desired composition point does not belong to H_1, but $T_2(\check{T}_2)$ has a point of intersection with H_2, then the composition of any intersection point of $T_2(\check{T}_2)$ and H_2 can be used as the feed of a CSTR (PFR) which delivers the desired composition as its exit, and this composition can be obtained by mixing the feed, product(s) of a CSTR and/or a PFR from the feed and the desired composition. The cross-flowrates of the reactor network can be obtained from the solution of balance equations (38)–(46) with known compositions, network inlet/outlet flowrates and finite reactors. A feasible solution of this problem is always guaranteed, as shown in Ref. [37], through the use of mixing ratios and subsequent identification of the reactor flowrates through solution of a set of linear independent equations, with equal number of unknowns and equations. If T_2 and $\check{T}_2$ do not intersect with H_2, the following can be used to identify a feasible reactor network. Let PU be the composition point union containing all extreme and interior grid points of the AR obtained from the Shrink-wrap algorithm excluding composition grid points contained by H_2. For the current PU:

(1) Select a composition grid point and let the convex hull defined by the selected point and H_2 be denoted as H_3 (a closed hull). If H_3 has no point of intersection with T_2 and $\check{T}_2$, a new PU is generated by eliminating the selected point from the current PU and starting over.
(2) Otherwise, let the backward CSTR (PFR) trajectories at the composition of the selected point, excluding the selected point itself, be denoted as $T_3(\check{T}_3)$. If either T_3 or $\check{T}_3$ has no point of intersection with H_3, a new PU is generated by eliminating the selected point from the current PU and starting over.
(3) Otherwise, any intersection point of H_3 and $T_2(\check{T}_2)$ can be used as the feed of a CSTR (PFR) which delivers the desired composition as its exit; and any intersection point of H_3 and $T_3(\check{T}_3)$ can be used as the feed of another CSTR (PFR) which delivers the composition of the selected point as its exit. The selected intersection points of H_3 and $T_2(\check{T}_2)$, and H_3 and $T_3(\check{T}_3)$ can be obtained by mixing the feed, product(s) of a CSTR and/or a PFR from the feed, the desired composition and the composition of the selected grid point. As before, the cross-flowrates of the reactor network can be obtained from the solution of balance equations (38)–(46) with known compositions, network inlet/outlet flowrates and finite reactors.

If selecting one point at a time from the PU does not succeed, then selecting two (or more) points at a time can be used, and the process can be continued until a reactor network that delivers the desired composition as its exit is identified. From the Shrink-wrap algorithm, it is guaranteed that a reactor network with a finite number of reactors can be identified to deliver any composition point in the AR as its exit, although it is possible that, all extreme points defining the AR may need to be used. However, practical experience suggests that the procedure succeeds in its early stages, and this is illustrated in the case studies. It is also important to point out that the procedure is applicable to both constant density and variable density AR's, in concentration space and mass fraction space, respectively.

4. Case studies

In this section, IDEAS is employed to identify the VDF AR for three gas phase reaction case studies. Reactors are presumed to be isothermal and isobaric. All computational efforts are carried out on a Linux machine with an AMD 2400+ MP cpu running at 2 GHz clock speed.

4.1. Trambouze reaction kinetics

Consider the following Trambouze-like gas phase reaction pathway taking place in an isothermal, isobaric reactor network, where $P = 56$ atm, $T = 550$ K. The feed is pure reactant A_1, and we seek to create the AR for components A_1 and A_3 in mass fraction space under the condition that gases are considered to be ideal.

$$A_1(\text{gas}) \xrightarrow{k_1} A_2(\text{gas}) \ (\text{zeroth order}, k_1 = 0.025\,\text{kmol}/(\text{m}^3\,\text{s})),$$

$$A_1 \xrightarrow{k_2} 2A_3 \ (\text{gas, product}) \ (\text{first order}, k_2 = 0.2(1/\text{s})),$$

$$A_1 \xrightarrow{k_3} A_4(\text{gas}) \ (\text{second order}, k_3 = 0.4\,\text{m}^3/(\text{kmol s}))$$

Molecular weight $M_1 = 40$ kg/kmol. The component generation rates for this reaction scheme are

$$r_1 = -k_1 - k_2 C_1 - k_3 C_1^2; \qquad r_2 = k_1;$$

$$r_3 = 2k_2 C_1; \qquad r_4 = k_3 C_1^2$$

First we derive the relations of component concentrations and mass fractions (i.e. Eqs. (20) and (31)). Since

$$C_1 = Cx_1, \quad C_3 = Cx_3; \qquad x_1 = \bar{M} z_1 \frac{1}{M_1}, \quad x_3 = \bar{M} z_3 \frac{1}{M_3};$$

$$\bar{M} = \frac{1}{(z_1/M_1) + (z_2/M_2) + (z_3/M_3) + (z_4/M_4)};$$

$$M_1 = M_2 = M_4 = 2M_3, \quad z_1 + z_2 + z_3 + z_4 = 1$$

it then holds:

$$C_1 = C \frac{z_1}{1+z_3}; \qquad C_3 = C \frac{2z_3}{1+z_3} \tag{53}$$

where C, $\bar{M}$ are the total concentration and the average molecular weight, respectively, and x_i and z_i are molar fraction and mass fraction for the ith component, respectively. In addition, based on the isothermal, isobaric and ideal gas assumptions, $C = P/RT = C^\circ = 1.237\,\text{kmol/m}^3$. As a result, Eq. (53) become:

$$C_1 = C^\circ \frac{z_1}{1+z_3}; \qquad C_3 = C^\circ \frac{2z_3}{1+z_3} \tag{54}$$

Since the generation rates for components A_1 and A_3 depend solely on z_1 and z_3, the VDF mass fraction/flowrate CSTR/PFR models for this case take the form.

CSTR model

$$z_1^{\hat{O}}(i) - z_1^{\hat{I}}(i) = \sigma(i) M_1 \left(-k_1 - k_2 C^\circ \frac{z_1^{\hat{O}}(i)}{1+z_3^{\hat{O}}(i)} - k_3 \left(C^\circ \frac{z_1^{\hat{O}}(i)}{1+z_3^{\hat{O}}(i)} \right)^2 \right) \tag{55}$$

$$z_3^{\hat{O}}(i) - z_3^{\hat{I}}(i) = \sigma(i) M_3 \left(2k_2 C^\circ \frac{z_1^{\hat{O}}(i)}{1+z_3^{\hat{O}}(i)} \right),$$

$$\text{if } \lambda(i) = 1, \quad \forall i = 1, \ldots, L \tag{56}$$

PFR model

$$\frac{dz_1}{d\bar{\sigma}} = M_1 \left(-k_1 - k_2 C^\circ \frac{z_1}{1+z_3} - k_3 \left(C^\circ \frac{z_1}{1+z_3} \right)^2 \right);$$

$$z_1|_{\bar{\sigma}=0} = z_1^{\hat{I}}(i), \quad z_1|_{\bar{\sigma}=\sigma(i)} = z_1^{\hat{O}}(i) \tag{57}$$

$$\frac{dz_3}{d\bar{\sigma}} = M_3 \left(2k_2 C^\circ \frac{z_1}{1+z_3} \right); \qquad z_3|_{\bar{\sigma}=0} = z_3^{\hat{I}}(i),$$

$$z_3|_{\bar{\sigma}=\sigma(i)} = z_3^{\hat{O}}(i), \quad \text{if } \lambda(i) = 0, \quad \forall i = 1, \ldots, L \tag{58}$$

As a result, the IDEAS formulation for a L-size finite dimensional approximation program can be summarized as follows:

$$q^{\text{I}} = \{q^{\text{I}}(1)\}, \quad z^{\text{I}} = \{z^{\text{I}}(1)\} = \{[\, z_1^{\text{I}}(1) \quad z_3^{\text{I}}(1)\,]^{\text{T}}\};$$

$$q^{\text{O}} = \{q^{\text{O}}(1)\}, \quad z^{\text{O}} = \{z^{\text{O}}(1)\} = \{[\, z_1^{\text{O}}(1) \quad z_3^{\text{O}}(1)\,]^{\text{T}}\};$$

$$q^{\hat{O}} = \{q^{\hat{O}}(1), q^{\hat{O}}(2), \ldots, q^{\hat{O}}(L)\},$$

$$z^{\hat{O}} = \{z^{\hat{O}}(1), z^{\hat{O}}(2), \ldots, z^{\hat{O}}(L)\};$$

$$z^{\hat{O}}(j) = [\, z_1^{\hat{O}}(j) \quad z_3^{\hat{O}}(j)\,]^{\text{T}}, \quad q^{\hat{I}} = \{q^{\hat{I}}(1), q^{\hat{I}}(2), \ldots, q^{\hat{I}}(L)\};$$

$$z^{\hat{I}} = \{z^{\hat{I}}(1), z^{\hat{I}}(2), \ldots, z^{\hat{I}}(L)\}, \quad z^{\hat{I}}(i) = [\, z_1^{\hat{I}}(i) \quad z_3^{\hat{I}}(i)\,]^{\text{T}}$$

Fig. 2 shows the result of the IDEAS computation, and Fig. 3 shows a reaction network, obtained by employing the procedure stated in Section 3.3, to achieve the maximum mass fraction of the product A_3.

The dot–dash curves are results in mass fraction space, when the constant density and isothermal operation assumptions are employed (no longer isobaric condition). Indeed, when the fluid density is constant, the following holds:

$$C_1 + C_2 + \frac{1}{2}C_3 + C_4 = C_1^0 \Rightarrow C - \frac{1}{2}C_3 = C^0 \tag{59}$$

as compared to the relation $C = C^0$ which holds for the variable density fluid. Combining Eq. (59) with Eq. (54), which holds for both the CDF and VDF cases, we get the following relations under the constant density assumption:

$$z_1 = \frac{C_1}{C^0}; \qquad z_3 = \frac{C_3}{2C^0} \tag{60}$$

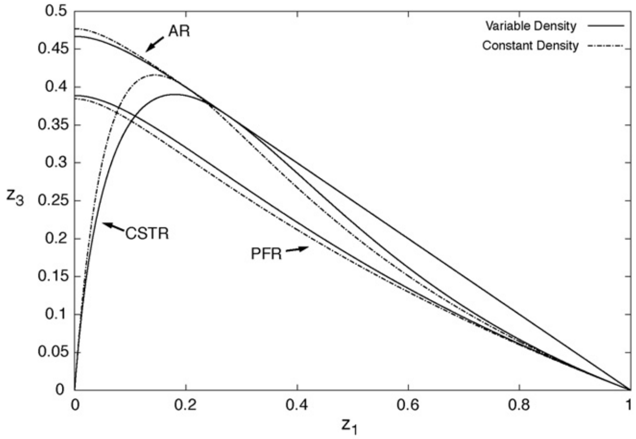

Fig. 2. Trambouze reaction kinetics attainable region in mass fraction space.

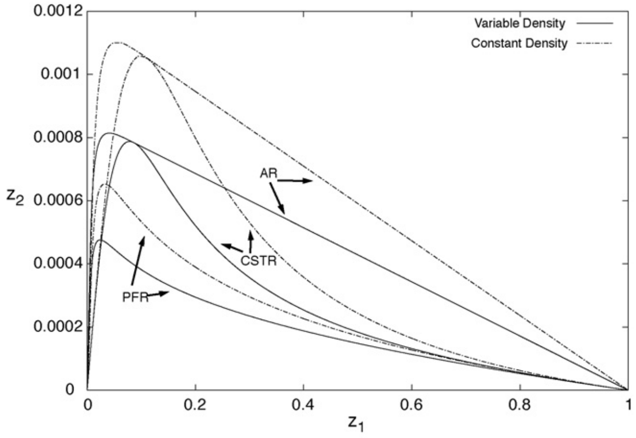

Fig. 4. Van de Vusse reaction kinetics attainable region in mass fraction space.

With these expressions, the Shink-wrap algorithm is carried out to construct the AR in mass fraction space for the CDF reactor network.

It can be seen from Fig. 2 that the constant density AR contains higher mass fraction values for product A_3, than when the variability of density is properly accounted for. The variable density AR boundary consists of a straight line that is tangent to the VDF CSTR curve and goes through the network feed, and a VDF PFR trajectory starting at the previously identified tangent point. This behavior is similar to that exhibited by the constant density AR. It can be seen from Fig. 3 that the maximum A_3 component mass fraction can be obtained by a reactor network that consists of a VDF CSTR followed by a VDF PFR. In the identification procedure, the desired composition point corresponding to maximum A_3 mass fraction (i.e. $(z_1, z_3) = (0.0, 0.467)$) does not belong to T_1 and $\check{T}_1$, and does not belong to H_1. However, the PFR backward trajectory from the desired composition point (i.e. $\check{T}_2$) intersects with H_2. Indeed, $\check{T}_2$ intersects with T_1. To this point, the procedure succeeds and the reactor network in Fig. 3 is identified.

4.2. Reversible Van de Vusse reaction kinetics

Let us consider the following Van de Vusse-like gas phase reaction pathway taking place in an isothermal, isobaric reactor network, with a feed of pure reactant A_1 and $C_1^0 = 2.0\,\text{kmol/m}^3$. We seek to create the AR for components A_1 and A_2 in mass fraction space again employing the ideal gas assumption.

$$A_1(\text{gas}) \xrightarrow{k_1} A_2\,(\text{gas, product})$$

$$(\text{first order}, k_1 = 1.0 \times 10^{-4}\,(1/\text{s}));$$

$$A_2 \xrightarrow{k_2} A_1\ (\text{first order}, k_2 = 5.0 \times 10^{-3}\,(1/\text{s}));$$

$$2A_2 \xrightarrow{k_3} A_3(\text{gas})\ (\text{second order}, k_3 = 2.0 \times 10^{-3}\,\text{m}^3/(\text{kmol s}));$$

$$2A_1 \xrightarrow{k_4} A_4(\text{gas})\ (\text{second order},\ k_4 = 0.2\,\text{m}^3/(\text{kmol s}))$$

where the molecular weight is $M_1 = 25$ kg/kmol. The reaction rates for this reaction pathway are given as

$$r_1 = -k_1C_1 + k_2\,C_2 - k_4C_1^2; \qquad r_2 = k_1C_1 - k_2C_2 - k_3C_2^2;$$

$$r_3 = \frac{1}{2}k_3\,C_2^2; \qquad r_4 = \frac{1}{2}k_4C_1^2$$

Again $C = P/RT = C^\circ = 2.0\,\text{kmol/m}^3$. The following relations can be easily derived:

$$C_1 = C\frac{2z_1}{1+z_1+z_2} = C^\circ\,\frac{2z_1}{1+z_1+z_2};$$

$$C_2 = C\frac{2z_2}{1+z_1+z_2} = C^\circ\frac{2z_2}{1+z_1+z_2} \tag{61}$$

The generation rates for components A_1 and A_2 depend solely on z_1 and z_2, the VDF mass fraction/flowrate models and the IDEAS formulation can be rewritten in the way similar to the above case, and is not elaborated here.

Fig. 4 shows the result of the IDEAS computation, and Fig. 5 shows a reaction network that achieves the maximum mass fraction of the product A_2.

When the density is constant, the following holds:

$$C_1 + C_2 + 2\,C_3 + 2\,C_4 = C_1^0 \Rightarrow 2\,C - C_1 - C_2 = C^0 \tag{62}$$

Combining with Eq. (61), we get

$$z_1 = \frac{C_1}{C^0}; \qquad z_2 = \frac{C_2}{C^0} \tag{63}$$

Again, the constant density AR attains higher product A_2 mass fraction values. However, close to the ordinate axis, the variable density AR contains points that are outside of the constant density AR.

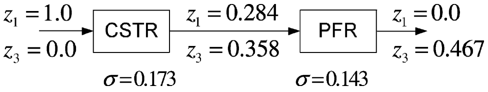

Fig. 3. Reactor configuration for trambouze reaction kinetics.

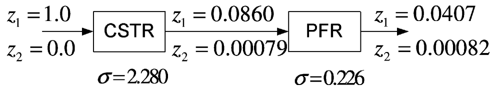

Fig. 5. Reactor configuration for Van de Vusse reaction kinetics.

4.3. Trambouze reaction kinetics revisited: no ideal gas assumption

In this case, we consider that the ideal gas law is not applicable and take into account the non-ideal behavior of the gases involved.

There are a number of non-ideal thermodynamic property models that can be used to capture non-ideal gas behavior. In this case study, a generalized compressibility factor equation of state is considered to capture the non-ideal behavior of all gases involved as follows:

$$C = \frac{1}{\mathcal{Z}} \frac{P}{RT} \tag{64}$$

where $\mathcal{Z}$ is the compressibility factor. This equation is suitable for both pure substances and mixtures. $\mathcal{Z}$ could be determined from experimental data, or other non-ideal thermodynamic models as well. Here, the Redlich-Kwong (R-K) equation is used:

$$R-K\text{ equation}: \quad P = \frac{RT}{(1/C)-b} - \frac{a}{(1/C)^2 + b(1/C)} \tag{65}$$

where $1/C$ is the molar volume, a and b are two species-dependent constants that can be estimated from the critical temperature, critical pressure and operating temperature. Combining the compressibility factor equation and the R-K equation, we have:

$$\mathcal{Z}^3 - \mathcal{Z}^2 + \left(\frac{aP - bPRT - b^2P^2}{R^2T^2}\right)\mathcal{Z} - \frac{abP^2}{R^3T^3} = 0 \tag{66}$$

The equation can be solved analytically for three roots. If there are multiple real roots, then the largest value of $\mathcal{Z}$ corresponds to the vapor phase, and the smallest value of $\mathcal{Z}$ corresponds to the liquid phase [38].

To apply the R-K equation to mixtures, mixing rules are used to average the constants a_i and b_i for each component in the mixture as follows:

$$a = \sum_{i=1}^{n}\left(\sum_{j=1}^{n} x_i x_j (a_i a_j)^{0.5}\right); \qquad b = \sum_{i=1}^{n} x_i b_i, \tag{67}$$

and

$$a_i = 0.42748 \frac{R^2 T_{ci}^{2.5}}{P_{ci} T^{0.5}}; \qquad b_i = 0.08664 \frac{RT_{ci}}{P_{ci}} \tag{68}$$

where T_{ci} and P_{ci} are the critical temperature and pressure for the ith species.

Since a mixture's compressibility factor $\mathcal{Z}$ is a function of all x_i and subsequently all z_i, the generation rates for components A_1 and A_3 no longer depend solely on z_1 and z_3, but on all z_i. The VDF mass fraction/flowrate CSTR/PFR models and the IDEAS formulation variables are given in the Appendix A for readers' convenience. The critical temperatures and pressures are given in Table 2. The three-dimensional (z_1, z_3, z_4) VDF AR is shown in Fig. 6, while its projection on the two-dimensional (z_1, z_3) subspace is shown in Fig. 7.

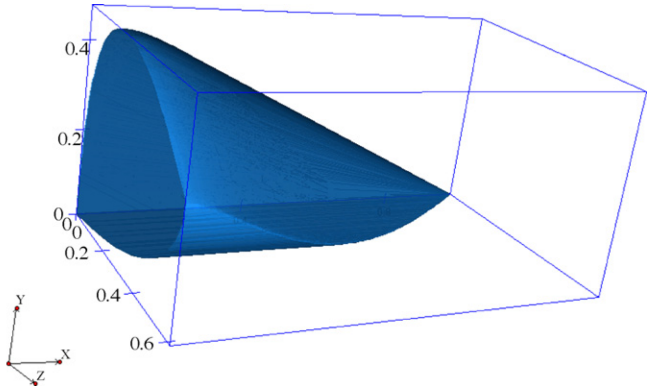

Fig. 6. Trambouze kinetics AR in 3D mass fraction space (no ideal gas assumption) x: z_1; y: z_2; z: z_3;

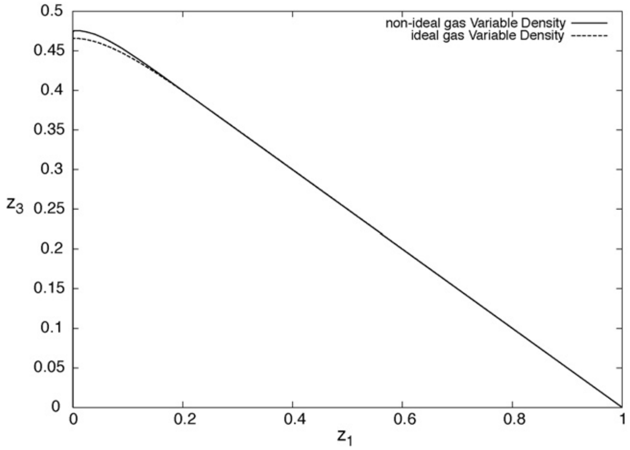

Fig. 7. Projection of Trambouze kinetics AR to (z_1, z_3) mass fraction space (no ideal gas assumption).

Table 2
Thermodynamic data

ith component	Critical temperature T_{ci} (K)	Critical pressure P_{ci} (kPa)
A_1	544	5030
A_2	538	4950
A_3	460	3500
A_4	548	5090

From Fig. 7, it can be seen that the non-ideal gas AR is larger than the ideal gas AR. This can be explained as follows: the calculation of $\mathcal{Z}$ using the above thermodynamic data ranges from 0.25 to 0.65 for the considered T, P conditions ($T = 550$ K, $P = 56$ atm). In turn, this gives rise to a higher average total molar concentration than the one arising under the ideal gas assumption. As a result, more A_3 is produced. The quantified peak mass fractions of product A_3 are 0.467 and 0.48 for the ideal gas AR and the non-ideal gas AR, respectively. Fig. 8 shows a

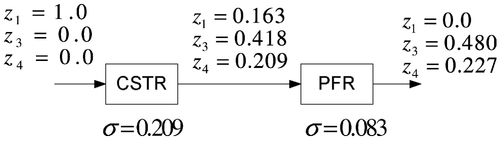

Fig. 8. Reactor configuration for Trambouze reaction kinetics without ideal gas assumption.

reaction network that achieves the maximum mass fraction of the product A_3.

5. Discussion and conclusions

In this work, the VDF CSTR and PFR models are shown to satisfy the requirements necessary for the application of the IDEAS framework to VDF reactor network synthesis problems (e.g. gas phase reactions). In addition, the Shrink-wrap algorithm for AR construction is shown to be applicable to VDF AR construction in mass fraction space. This conceptual development allows the rigorous application of the Shrink-wrap AR construction methodology in mass fraction space to VDF reactor networks. The proposed methodology is illustrated on three case studies, involving both ideal and non-ideal gas models.

Future research will focus on the synthesis of non-isothermal VDF reactor networks. By incorporating energy balance equations in each reactor model, and demonstrating again the applicability of IDEAS, non-isothermal VDF reactor network synthesis problems can be addressed, albeit in higher dimensional spaces than those used for isothermal problems.

Acknowledgments

The authors gratefully acknowledge financial support from the National Science Foundation through grant CTS 0301931 and the equipment donated by Intel Corporation through its Higher Education Program.

Appendix A. VDF models and IDEAS variables for Trambouze reaction kinetics without ideal gas assumption

The VDF mass fraction/flowrate CSTR/PFR models.

CSTR model

$$z_1^{\hat{O}}(i) - z_1^{\hat{I}}(i) = \sigma(i)M_1(-k_1 - k_2Cx_1 - k_3(Cx_1)^2) \quad (69)$$

$$z_3^{\hat{O}}(i) - z_3^{\hat{I}}(i) = \sigma(i)M_3(2k_2(Cx_1)) \quad (70)$$

$$z_4^{\hat{O}}(i) - z_4^{\hat{I}}(i) = \sigma(i)M_4(k_3(Cx_1)^2) \quad (71)$$

$$C = \frac{1}{\mathcal{Z}}\frac{P}{RT} \quad (72)$$

$$\mathcal{Z}^3 - \mathcal{Z}^2 + \left(\frac{aP - bPRT - b^2P^2}{R^2T^2}\right)\mathcal{Z} - \frac{abP^2}{R^3T^3} = 0 \quad (73)$$

$$a = \sum_{i=1}^{4}\left(\sum_{j=1}^{4} x_ix_j(a_ia_j)^{0.5}\right); \qquad b = \sum_{i=1}^{4} x_ib_i \quad (74)$$

$$x_1 = \frac{z_1(i)}{1 + z_3(i)}; \qquad x_3 = \frac{2z_3(i)}{1 + z_3(i)}; \qquad x_4 = \frac{z_4(i)}{1 + z_3(i)} \quad (75)$$

$$x_2 = 1 - x_1 - x_3 - x_4, \quad \text{if } \lambda(i) = 1, \quad \forall i = 1, \ldots, L \quad (76)$$

PFR model

$$\frac{dz_1}{d\bar{\sigma}} = M_1(-k_1 - k_2Cx_1 - k_3(Cx_1)^2);$$

$$z_1|_{\bar{\sigma}=0} = z_1^{\hat{I}}(i), \quad z_1|_{\bar{\sigma}=\sigma(i)} = z_1^{\hat{O}}(i) \quad (77)$$

$$\frac{dz_3}{d\bar{\sigma}} = M_3(2k_2(Cx_1));$$

$$z_3|_{\bar{\sigma}=0} = z_3^{\hat{I}}(i), \quad z_3|_{\bar{\sigma}=\sigma(i)} = z_3^{\hat{O}}(i) \quad (78)$$

$$\frac{dz_4}{d\bar{\sigma}} = M_4(k_3(Cx_1)^2);$$

$$z_4|_{\bar{\sigma}=0} = z_4^{\hat{I}}(i), \quad z_4|_{\bar{\sigma}=\sigma(i)} = z_4^{\hat{O}}(i) \quad (79)$$

$$C = \frac{1}{\mathcal{Z}}\frac{P}{RT} \quad (80)$$

$$\mathcal{Z}^3 - \mathcal{Z}^2 + \left(\frac{aP - bPRT - b^2P^2}{R^2T^2}\right)\mathcal{Z} - \frac{abP^2}{R^3T^3} = 0 \quad (81)$$

$$a = \sum_{i=1}^{4}\left(\sum_{j=1}^{4} x_ix_j(a_ia_j)^{0.5}\right); \qquad b = \sum_{i=1}^{4} x_ib_i \quad (82)$$

$$x_1 = \frac{z_1}{1 + z_3}; \qquad x_3 = \frac{2z_3}{1 + z_3}; \qquad x_4 = \frac{z_4}{1 + z_3} \quad (83)$$

$$x_2 = 1 - x_1 - x_3 - x_4, \quad \text{if } \lambda(i) = 0, \quad \forall i = 1, \ldots, L \quad (84)$$

The IDEAS formulation for a L-size finite dimensional approximation program can be summarized as follows:

$$q^{\mathrm{I}} = \{q^{\mathrm{I}}(1)\}, \quad z^{\mathrm{I}} = \{z^{\mathrm{I}}(1)\} = \{[\, z_1^{\mathrm{I}}(1) \quad z_3^{\mathrm{I}}(1) \quad z_4^{\mathrm{I}}(1)\,]^{\mathrm{T}}\};$$

$$q^{\mathrm{O}} = \{q^{\mathrm{O}}(1)\}, \quad z^{\mathrm{O}} = \{z^{\mathrm{O}}(1)\} = \{[\, z_1^{\mathrm{O}}(1) \quad z_3^{\mathrm{O}}(1) \quad z_4^{\mathrm{O}}(1)\,]^{\mathrm{T}}\};$$

$$q^{\hat{O}} = \{q^{\hat{O}}(1), q^{\hat{O}}(2), \ldots, q^{\hat{O}}(L)\};$$

$$z^{\hat{O}} = \{z^{\hat{O}}(1), z^{\hat{O}}(2), \ldots, z^{\hat{O}}(L)\},$$

$$z^{\hat{O}}(j) = [\, z_1^{\hat{O}}(j)z_3^{\hat{O}}(j) \quad z_4^{\hat{O}}(j) \quad]^{\mathrm{T}};$$

$$q^{\hat{I}} = \{q^{\hat{I}}(1), q^{\hat{I}}(2), \ldots, q^{\hat{I}}(L)\};$$

$$z^{\hat{I}} = \{z^{\hat{I}}(1), z^{\hat{I}}(2), \ldots, z^{\hat{I}}(L)\},$$

$$z^{\hat{I}}(i) = [\, z_1^{\hat{I}}(i) \quad z_3^{\hat{I}}(i) \quad z_4^{\hat{I}}(i)\,]^{\mathrm{T}}$$

References

[1] G. Gavalas, Nonlinear Differential Equations of Chemically Reacting Systems: Springer Tracts in Natural Philosophy, vol. 17, Springer, New York, 1968.

[2] O. Levenspiel, Chemical Reaction Engineering, Wiley, New York, 1972.

[3] G. Froment, K. Bischof, Chemical Reactor Analysis and Design, Wiley, New York, 1979.

[4] H.S. Fogler, Elements of Reaction Engineering, 3rd ed., Prentice-Hall, New Jersey, 1999.

[5] L. Schmidt, Engineering of Chemical Reactions, Oxford University Press, North Carolina, 1998.

[6] J. Rawlings, J. Ekerdt Chemical Reactor Analysis and Design Fundamentals, Nob Hill Publishing, Wisconsin, 2002.

[7] R. Jackson, Optimization of chemical reactors with respect to flow configuration, J. Optim. Theory Appl. 2 (1968) 240.

[8] A.L. Ravimohan, Optimization of chemical reactor networks with respect to flow configuration, J. Optim. theory Appl. 8 (1968) 204.

[9] J.D. Paynter, D.E. Haskins, Determination of optimal reactor type, Chem. Eng. Sci. 25 (1970) 1415.

[10] S.L. Ong, Optimization of CSTRs in series by dynamic programming, Biotechnol. Bioeng. 28 (1986) 818.

[11] L. Achenie, L.T. Biegler, Algorithmic synthesis of chemical reactor networks using mathematical programming, Ind. Eng. Chem. Res. 25 (1986) 621.

[12] L. Achenie, L.T. Biegler, Developing targets for the performance index of a chemical reactor network: isothermal systems, Ind. Eng. Chem. Res. (1988) 1811–1821.

[13] L. Achenie, L.T. Biegler, A superstructure based approach to chemical reactor network synthesis, Comput. Chem. Eng. 14 (1990) 23.

[14] A.C. Kokossis, C.A. Floudas, Optimization of complex reactor networks. I. Isothermal operation, Chem. Eng. Sci. 45 (1990) 595.

[15] A.C. Kokossis, C.A. Floudas, Optimization of complex reactor networks. II. Nonisothermal operation, Chem. Eng. Sci. 49 (1994) 1037.

[16] E.C. Marcoulaki, A.C. Kokossis, Scoping and screening complex reaction networks using stochastic optimization, AIChE J. 45 (1999) 1977.

[17] V.L. Mehta, A.C. Kokossis, Nonisothermal synthesis of homogeneous and multiphase reactor networks, AIChE J. 46 (2000) 2256.

[18] M. Hillestad, A systematic generatioin of reactor designs. I. Isothermal conditions, Comput. Chem. Eng. 28 (2004) 2717.

[19] F. Horn, Attainable and non-attainable regions in chemical reactor technique, in: Third European Symposium on Chemical Reaction Engineering, Pergamon Press, London, 1964, pp. 123–138.

[20] D. Glasser, D. Hildebrandt, C. Crowe, A geometric approach to steady flow reactors: the attainable region and optimization in concentration space, Ind. Eng. Chem. Res. 26 (1987) 1803.

[21] D. Hildebrandt, D. Glasser, C. Crowe, Geometry of the attainable region generated by reaction and mixing: with and without constraints, Ind. Eng. Chem. Res. 29 (1990) 49.

[22] D. Glasser, D. Hildebrandt, S. Godorr, The attainable region for segregated maximum mixed and other reactor models, Ind. Eng. Chem. Res. 33 (1994) 1136.

[23] S. Godorr, D. Hildebrandt, D. Glasser, C. McGregor, Choosing optimal control policies using the attainable region approach, Ind. Eng. Chem. Res. 38 (1999) 639.

[24] D. Hildebrandt, L.T. Biegler, Synthesis of chemical reactor networks, in: Proceedings of the Fourth International Conference on Foundations of Computer-Aided Process Design, 1995, pp. 52–67, AIChE.

[25] S. Balakrishna, L.T. Biegler, Constructive targeting approaches for the synthesis of chemical reactor networks, Ind. Eng. Chem. Res. 31 (1992) 300.

[26] M. Feinberg, Recent results in optimal reactor synthesis via attainable region theory, Chem. Eng. Sci. 54 (1999) 2535.

[27] M. Feinberg, Optimal reactor design from a geometric viewpoint. Part II. critical sidestream reactors, Chem. Eng. Sci. 55 (2000) 2455.

[28] M. Feinberg, Optimal reactor design from a geometric viewpoint. Part III. critical CFSTRs, Chem. Eng. Sci. 55 (2000) 3553.

[29] M. Feinberg, D. Hildebrandt, Optimal reactor design from a geometric viewpoint. I. Universal properties of the attainable region, Chem. Eng. Sci. 52 (1997) 1637.

[30] S. Wilson, V. Manousiouthakis, IDEAS approach to process network sythesis: application to multicomponent MEN, AIChE J. 46 (2000) 2408.

[31] J.F. Burri, S.D. Wilson, V.I. Manousiouthakis, Infinite DimEnsionAl State-space (IDEAS) approach to reactor network synthesis: application to attainable region construction, Comput. Chem. Eng. 26 (2002) 849.

[32] J. Drake, V.I. Manousiouthakis, IDEAS approach to process network synthesis: minimum plate area for complex distillation networks with fixed utility cost, Ind. Eng. Chem. Res. 41 (2002) 4984.

[33] J. Drake, V.I. Manousiouthakis, IDEAS approach to process network synthesis: minimum utility cost for complex distillation networks, Chem. Eng. Sci. 57 (2002) 3095.

[34] A.M. Justanieah, V.I. Manousiouthakis, IDEAS approach to separation network synthesis: application to chromium recovery from wastewater, Adv. Environ. Res. 7 (2003) 549.

[35] L.L. Martin, V.I. Manousiouthakis, Globally optimal power cycle synthesis via the Infinite-DimEnsionAl State-space (IDEAS) approach featuring minimum area with fixed utility, Chem. Eng. Sci. 58 (2003) 4291.

[36] S. Kauchali, W.C. Rooney, L.T. Biegler, D. Glasser, D. Hildebrandt, Linear programming formulations for attainable region analysis, Chem. Eng. Sci. 57 (2002) 2015.

[37] V.I. Manousiouthakis, A.M. Justanieah, L.A. Taylor, The Shrink-wrap algorithm for the construction of the attainable region: application of the IDEAS framework, Comput. Chem. Eng. 28 (2004) 1563–1575.

[38] J.D. Seader, E.J. Henley, Separation Process Principles, Johe Wiley & Sons Inc., 1998.